THE JOURNAL OF PHYSICAL CHEMISTRY C

Article

pubs.acs.org/JPCC

Proton-Induced Dysfunction Mechanism of Cathodes in an Aqueous Lithium Ion Battery

Qiang Shu,[†] Long Chen,[‡] Yongyao Xia,[‡] Xingao Gong,[†] and Xiao Gu*[,§]

[†]Key Laboratory of Computational Physical Sciences, Ministry of Education, State Key Laboratory of Surface Physics, and Department of Physics, [‡]Department of Chemistry, Shanghai Key Laboratory of Molecular Catalysis and Innovative Materials, Institute of New Energy, and [§]Key Laboratory of Computational Physical Sciences, Ministry of Education, Department of Environmental Sciences and Engineering, Fudan University, Shanghai 200433, China

Supporting Information

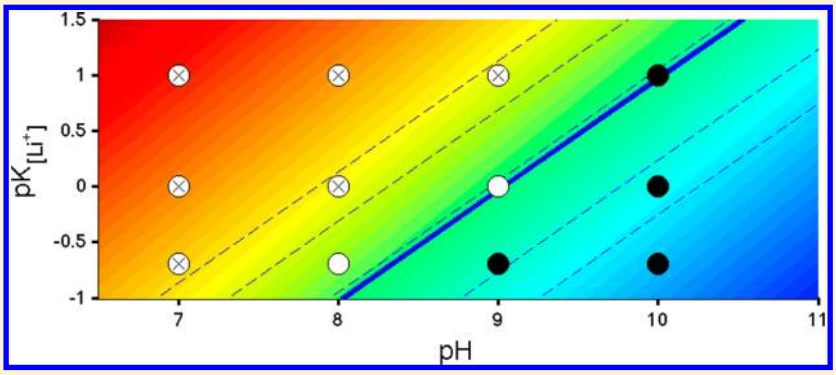

ABSTRACT: The proton-induced dysfunction mechanism of cathodes in aqueous lithium ion batteries is investigated by combining both experimental and theoretical research. We have found the electrochemical stability of the cathodes in a Li^+-containing aqueous electrolyte solution is critically dependent on the pH value of the solution. The cyclic voltammograms of the cathodes show that the cathodes become dysfunctional when the pH of the solution decreases right below a certain value. We find that the competition reactions to the cathodes of the H^+ and Li^+ in the solution dominate whether Li^+ or H^+ would be intercalated. Thermodynamic analysis proves that the critical pH, which divide the normal and dysfunctional behaviors, is determined by both the difference of the binding energies of Li^+ and H^+ cations to the cathodes and the chemical potentials of the Li^+ and H^+ in the solution.

Lithium ion batteries (LIBs) have been proved to be commercially successful in various applications, triumphantly in portable devices.[1] Therefore, both scientific and engineering interests drive lots of research on the related areas.[2,3] In order to implement those high efficient cathodes into power suppliers in such as electric vehicles, the power efficiency required is rather higher than the portable devices. Aqueous electrolytes represent a promising avenue for tackling those problems. In 1994, Dahn et al. successfully assembled an aqueous LIB with VO_2 as the anode and $LiMn_2O_4$ as the cathode;[4,5] despite of that, the battery had a poor cycle life. Since then, the electrochemistry of compounds in an aqueous electrolyte had attracted increasing attention.[6−9] Only recently, the cycling stability was greatly improved by our research group.[10,11]

The critical factor that differs the aqueous solutions from the nonaqueous electrolytes is the action of the H^+, as the concentration of the H^+ ion (pH) is the key point in the performance of the cathodes.[12−14] The presence of the H^+ ion has enriched the potential reactions of aqueous LIBs in solutions.[15] For further improvements on the reliability and stability of the aqueous LIB, it is very important to understand the details of the relationship of H^+ and Li^+ in such an environment.

Since the H^+ is competitive with the working Li^+ in the reactions to the cathodes, we have analyzed the competition between the H^+ and Li^+. Such competitive reactions are found to dominate the dysfunction mechanism of cathodes in aqueous solutions upon cycling. We have combined first-principle calculations and electrochemistry experiments to understand the mechanism.

First-principles calculations are based on density functional theory (DFT). The general gradient approximation (GGA) of Perdew and Wang (PW91) was employed for the exchange-correlation functional.[16] The projector augmented wave (PAW) method was used to describe the interactions between the valence electrons and the ionic cores.[17] The wave functions were expanded in a plane wave basis truncated at a plane wave energy of 450 eV. Geometry optimizations were converged to a force cutoff of 0.01 eV/Å. In the calculations of layer-structure $LiCo^{1}/_{3}Ni^{1}/_{3}Mn^{1}/_{3}O_2$, a supercell containing 12 formula units is

Received: November 14, 2012
Revised: February 21, 2013

   dx.doi.org/10.1021/jp311270s | J. Phys. Chem. C XXXX, XXX, XXX−XXX

employed. The lattice for the supercell is $a = b = 5.72$ Å and $c = 14.08$ Å. The AFM configuration is set to be two "spin-up" and two "spin-down" in the same cobalt−nickel−manganese layer. The Ni, Co, and Mn atoms are distributed evenly in the layers.

In the discharging procession of an aqueous lithium battery, two competitive redox reactions on the cathodes would be expected when the cathodes $Li_x(MO)_y$ (MO = transition metal oxides) are still stable in the solution:

$$Li_x(MO)_y(s) + Li^+(aq) + e^- \rightarrow Li_{x+1}(MO)_y(s) \quad (R1)$$

$$Li_x(MO)_y(s) + H^+(aq) + e^- \rightarrow HLi_x(MO)_y(s) \quad (R2)$$

Reaction R1 is the reaction of normal lithium intercalations and reaction R2 is the reaction where H^+ replaces the lithium ion to be intercalated. H^+ in the cathodes like spinel $LiMn_2O_4$ and $LiCoO_2$ have been reported.[18] H^+ always likes to be attached to an oxygen ion with hydrogen−oxygen chemical bonds.[19,20] In all of our samples, the pH values of the solutions are all above 7. Here, in reactions R1 and R2, the chemical potentials change:

$$\mu_{Li_x(MO)_y(s)} + \mu_{Li^+(aq)} + \mu_{e^-} = \mu_{Li_{x+1}(MO)_y(s)} + \Delta G_{Li^+} \quad (1)$$

$$\mu_{Li_x(MO)_y(s)} + \mu_{H^+(aq)} + \mu_{e^-} = \mu_{HLi_x(MO)_y(s)} + \Delta G_{H^+} \quad (2)$$

where

$$\mu_{Li^+(aq)} = \mu^0_{Li^+(aq)} + kT\ln[Li^+]; \quad \mu_{H^+(aq)} = \mu^0_{H^+(aq)} + kT\ln[H^+]$$

ΔG_{Li^+} and ΔG_{H^+} are the responsible chemical potentials differentials in the two reactions.

If the battery is working normally, the reaction of the Li^+ is required to release higher energy than the one of the H^+:

$$\Delta G_{Li^+} \geq \Delta G_{H^+} \quad (3)$$

According to eqs 1−3,

$$pH \geq \frac{\Delta}{kT\ln 10} - pK_{[Li^+]} \quad (3b)$$

where $\Delta = \mu^0_{H^+(aq)} - \mu^0_{HLi_x(MO)_y(s)} - \mu^0_{Li^+(aq)} + \mu^0_{Li_{x+1}(MO)_y(s)}$. This equation shows that the concentrations of the Li^+ and H^+ determine the intercalation competition between reactions R1 and R2. The battery works normally only when the H^+ concentration is below the pH value from eq 3b.

In order to get Δ, we employ two virtual reactions:

$$Li(atom) + Li_x(MO)_y(s) \rightarrow Li_{x+1}(MO)_y(s) \quad (R3)$$

$$H(atom) + Li_x(MO)_y(s) \rightarrow HLi_x(MO)_y(s) \quad (R4)$$

Reactions R3 and R4 both take place at standard conditions, 1 atm and 298.15 °C, where

$$\mu^0_{Li(atom)} + \mu^0_{Li_x(MO)_y(s)} = \mu^0_{Li_{x+1}(MO)_y(s)} + \Delta G_1$$

$$\mu^0_{H(atom)} + \mu^0_{Li_x(MO)_y(s)} = \mu^0_{HLi_x(MO)_y(s)} + \Delta G_2$$

Then,

$$\Delta = \mu^0_{H^+(aq)} - \mu^0_{H(atom)} - \mu^0_{Li^+(aq)} + \mu^0_{Li(atom)} + \Delta G_2 - \Delta G_1$$

For the simplicity, we now define

$$\Delta_1 = \mu^0_{H^+(aq)} - \mu^0_{H(atom)} - \mu^0_{Li^+(aq)} + \mu^0_{Li(atom)}$$

$$\Delta_2 = \Delta G_2 - \Delta G_1$$

Δ_1 could be calculated by the ionization energy of an atom and the hydration energy of an ion into water. The ionization energies for an atom and the hydration energies for ions have been widely studied by both theoretical and experimental methods.[21−23] We have now employed two results from ref 12, as listed in Table 1.

Table 1. Ionization Energies (E_{ion}) and Hydration Energies (E_{hyd}) for H and Li[a]

	E_{ion}	E_{hyd}	$E_{ion} + E_{hyd}$	E^{tot}	G^{corr}
H	13.6	−11.45[12]	2.15	−1.116	−0.012
Li	5.392	−5.487[12]	−0.0957	−0.2766	−0.013

[a]Calculated total energies for an atom (E^{tot}) calculated by VASP, and Gibbs free energy correction calculated by Gaussian. All units in eV.

$$\Delta_1 = \mu^0_{H^+(aq)} - \mu^0_{H(atom)} - \mu^0_{Li^+(aq)} + \mu^0_{Li(atom)}$$

$$= (E^{H^+}_{ion} + E^{H^+}_{hyd}) - (E^{Li^+}_{ion} + E^{Li^+}_{hyd}) = 2.245 \text{ eV}$$

Δ_2 is the partial mole free energy. In order to calculate the chemical potentials, we have carried out first-principle calculations for the total energies of the compounds. Gibbs free energies could be approximately calculated by first-principles methods according to reactions R3 and R4, by assuming Gibbs free energies of the bulk are a summation of their calculated total energies, the free energy part from vibrational entropy. The Gibbs free energies of the gaseous compounds are calculated by the total energy of an atom adding a correction term from the Gaussian calculation.

$$\Delta_2 = \Delta E + E_{corr} + \Delta F^{vib} \quad (4)$$

where $\Delta E = E^{tot}_{Li_{x+1}(MO)_y} - E^{tot}_{HLi_x(MO)_y}$

$$\Delta F^{vib} = (F^{vib}_{Li_{x+1}(MO)_y} - E^{vib}_{HLi_x(MO)_y})$$

(More details are in the Supporting Information.)

$$pH \geq \frac{2.245 + \Delta E + E_{corr} + \Delta F^{vib}}{kT\ln 10} - pK_{[Li^+]}$$

We have previously shown that the electrochemical stability of the layer-structured $LiCo^1/_3Ni^1/_3Mn^1/_3O_2$ is critically dependent upon the pH of the electrolyte solutions.[24] In low-pH solutions, these cathodes were unstable and lost their capacity upon a few cycles. The electrochemical stability of $LiCo^1/_3Ni^1/_3Mn^1/_3O_2$ cycling is comprehensively investigated using the powder microelectrode technique. Figure 1 shows the cyclic voltammograms (CVs) of $LiCo^1/_3Ni^1/_3Mn^1/_3O_2$ in aqueous electrolyte solutions with several pH values. Two samples, containing 0.1 and 5 M Li^+, respectively, are shown. In the 0.1 M Li^+ solution, the performance cycles decay quickly in pH = 7 solutions and become more stable in pH = 10 solution. Similar results are found in the 5 M Li^+ solutions, except that each performance decays slower. Actually, in the 5 M Li^+ solution, the CV becomes stable in pH = 9 solution. These voltammograms show that the electrochemical stability of $LiCo^1/_3Ni^1/_3Mn^1/_3O_2$ is critically dependent on the electrolyte pH and the concentration of the

dx.doi.org/10.1021/jp311270s | J. Phys. Chem. C XXXX, XXX, XXX−XXX

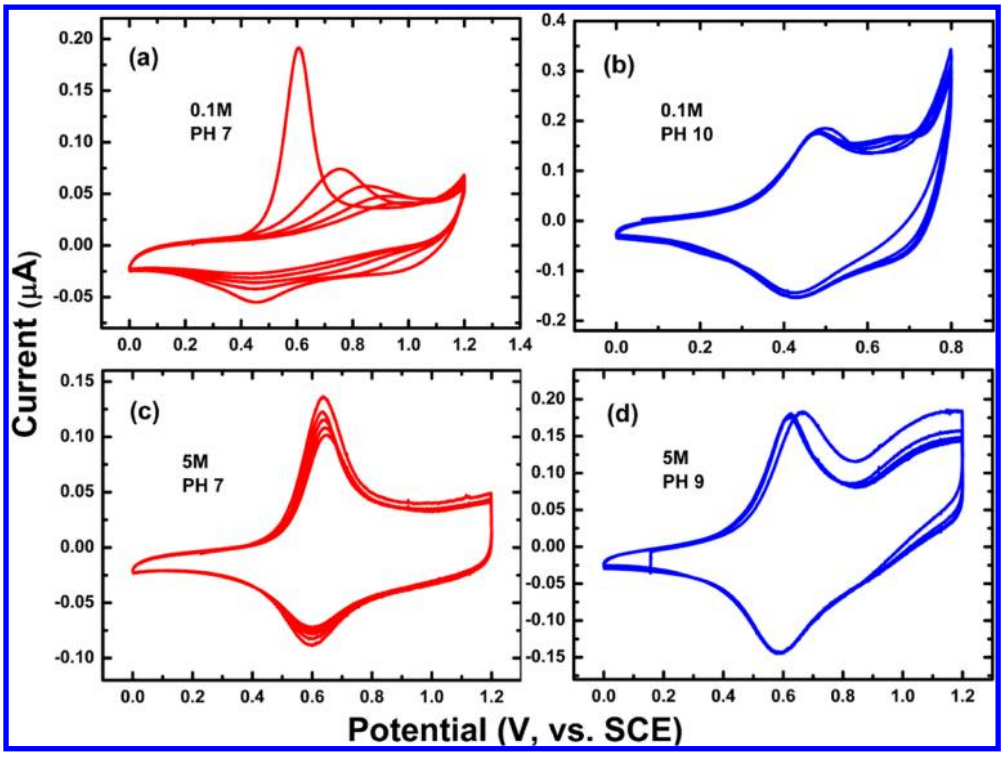

Figure 1. CVs of $LiCo^{1}/_{3}Ni^{1}/_{3}Mn^{1}/_{3}O_2$ in 0.1 and 5 M Li^+ aqueous solutions at various pH environments. The scan rate is 10 mV/s, and the voltages are from 0 to 1.1 V (vs SCE, the saturated calomel electrode). (a) 0.1 M, pH = 7; (b) 0.1 M, pH = 10; (c) 5 M, pH = 7; and (d) 5 M, pH = 9.

Li^+. The chemical instability in the low-pH electrolyte solutions is due to intercalation of the H^+.[25,26]

Table 2 lists the differences of the calculated total energies (ΔE) between the Li^+ and H^+ intercalated $LiCo_3Ni_3Mn_3O_{18}$.

Table 2. Calculated the Difference (ΔE) of the Total Energies between $HLi_xCo_3Ni_3Mn_3O_{18}$ and $Li_xCo_3Ni_3Mn_3O_{18}$

x	8	7	6	4	2
ΔE (eV)	−0.9	−0.78	−0.81	−0.86	−0.89

As eq 4 shows, the difference of the binding energies between the H^+ and Li^+ in cathodes dominates the competition reactions. We also noticed that ΔE is dependent on the concentration of the lithium ions in the cathodes especially at the discharging process. This means the competition actually varies with the depth of discharging.

Figure 2 shows the relations between the Li^+ and H^+ concentrations in the electrolyte. According to eq 3b, linear boundaries are found, where critical pK values are found according to the corresponding pH. The boundaries divide the normal performance and the ill performance of the cathodes as the pH and pK change. Since the ΔE value varies with the discharging depth, several lithium concentrations are considered, shown as the dashed lines in Figure 2. An averaged value of the ΔE is shown as the solid line, which gives the boundary of the cathodes.

We have also carried out quick investigations on the spinel $LiMn_2O_4$ and layer-structure $LiCoO_2$ cathodes. The H^+ and Li^+ share a larger energy difference in spinel $LiMn_2O_4$, which indicates that $LiMn_2O_4$ could tolerate larger H^+ concentration compared to $LiCo^{1}/_{3}Ni^{1}/_{3}Mn^{1}/_{3}O_2$. As a matter of fact, in spinel $LiMn_2O_4$, ΔE is also less violated by the lithium concentration.

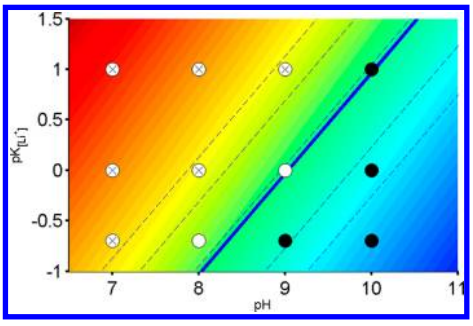

Figure 2. Critical $pK_{[Li^+]}$ for layer-structured $LiCo^{1}/_{3}Ni^{1}/_{3}Mn^{1}/_{3}O_2$ in aqueous solution as a function of the H^+ concentration. The dashed lines are the ones of the different discharging depths. The solid lines are the averaged value. Linear relations of the critical values divide the area into normal-working phase (down-side), and ill-performance phase (up-side). Experimental results are also shown as dots. Dots with a cross inside are ill performance, black dots are normal performance, and open dots are between ill and normal performance.

However, due to the size effect of the particles, the more complicity of the magnetism, and the stability to OH^- ions, the experimental CVs are much more complicated. However, we can still conclude that spinel $LiMn_2O_4$ is much stable in low pH solutions.

In conclusion, we have investigated the mechanism of the origin of the dysfunction mechanism of the cathodes: pH-dependent performance of the LIB in aqueous solutions. By combining first-principle calculations and electrochemical experiments, we have shown the critical pH values $LiCo^{1}/_{3}Ni^{1}/_{3}Mn^{1}/_{3}O_2$ for normal function in the aqueous electrolytes. We also found that spinel $LiMn_2O_4$ has the lowest pH value, which means $LiMn_2O_4$ can tolerant more H^+ in solution. The difference of binding energies of the H^+ and Li^+ has been found to be the key point.

dx.doi.org/10.1021/jp311270s | J. Phys. Chem. C XXXX, XXX, XXX−XXX

■ ASSOCIATED CONTENT

Supporting Information

Details on the competition reactions between Li^+ and H^+ into cathodes, details on the calculations, and the experimental CV data. This material is available free of charge via the Internet at http://pubs.acs.org.

■ AUTHOR INFORMATION

Corresponding Author

*Fax: (+86) 21-55655515; e-mail: gx@fudan.edu.cn.

Notes

The authors declare no competing financial interest.

■ ACKNOWLEDGMENTS

This work was partially supported by the Special Funds for Major State Basic Research, National Science Foundation of China, Ministry of Education and Shanghai municipality. The computation was performed in the Supercomputer Center of Shanghai, the Supercomputer Center of Fudan University.

■ REFERENCES

(1) Armstrong, A. R.; Bruce, P. G. Synthesis of Layered $LiMnO_2$ as an Electrode for Rechargeable Lithium Batteries. *Nature* **1996**, *381*, 499.

(2) Whittingham, M. S. Lithium Batteries and Cathode Materials. *Chem. Rev.* **2004**, *104*, 4271.

(3) Kang, K.; Meng, Y. S.; Bréger, J.; Grey, C. P.; Ceder, G. Electrodes with High Power and High Capacity for Rechargeable Lithium Batteries. *Science* **2006**, *311*, 977.

(4) Li, W.; Dahn, J. R.; Wainwright, D. S. Rechargeable Lithium Batteries with Aqueous Electrolytes. *Science* **1994**, *264*, 1115.

(5) Li, W.; Mckinnon, W. R.; Dahn, J. A. Lithium Intercalation from Aqueous Solutions. *J. Electrochem. Soc.* **1994**, *141*, 2310.

(6) Wang, G.; Fu, L.; Zhao, N.; Yang, L.; Wu, Y.; Wu, H. An Aqueous Rechargeable Lithium Battery with Good Cycling Performance. *Angew. Chem., Int. Ed.* **2007**, *46*, 295.

(7) Wang, G. X.; Zhong, S.; Bradhurst, D. H.; Dou, S. X.; Liu, H. K. Secondary Aqueous Lithium-Ion Batteries with Spinel Anodes and Cathodes. *J. Power Sources* **1998**, *74*, 198.

(8) Zhang, S.; Li, Y.; Wu, C.; Zheng, F.; Xie, Y. Novel Flowerlike Metastable Vanadium Dioxide (B) Micronanostructures: Facile Synthesis and Application in Aqueous Lithium Ion Batteries. *J. Phys. Chem. C* **2009**, *113*, 15058.

(9) Ruffo, R.; Wessells, C.; Huggins, R. A.; Cui, Y. Electrochemical Behavior of $LiCoO_2$ as Aqueous Lithium-Ion Battery Electrodes. *Electrochem. Commun.* **2009**, *11*, 247.

(10) Luo, J. Y.; Xia, Y. Y. Aqueous Lithium-Ion Battery $LiTi_2(PO_4)_3$/$LiMn_2O_4$ with High Power and Energy Densities as well as Superior Cycling Stability. *Adv. Funct. Mater.* **2007**, *17*, 3877.

(11) Luo, J. Y.; Cui, W. J.; He, P.; Xia, Y. Y. Raising the Cycling Stability of Aqueous Lithium-Ion Batteries by Eliminating Oxygen in the Electrolyte. *Nat. Chem.* **2010**, *2*, 760.

(12) Benedek, R.; van de Walle, A. Free Energies for Acid Attack Reactions of Lithium Cobaltate. *J. Electrochem. Soc.* **2008**, *155*, A711.

(13) Jayalakshmi, M.; Rao, M. M.; Scholz, F. Electrochemical Behavior of Solid Lithium Manganate ($LiMn_2O_4$) in Aqueous Neutral Electrolyte Solutions. *Langmuir* **2003**, *19*, 8403.

(14) Gu, X.; Liu, J. L.; Yang, J. H.; Xiang, H. J.; Gong, X. G.; Xia, Y. Y. First-Principles Study of H^+ Intercalation in Layer-Structured $LiCoO_2$. *J. Phys. Chem. C* **2011**, *115*, 12672.

(15) Zheng, J.; Chen, J. J.; Jia, X.; Song, J.; Wang, C.; Zheng, M. S.; Dong, Q. F. Electrochemical Performance of the $LiNi_{1/3}Co_{1/3}Mn_{1/3}O_2$ in Aqueous Electrolyte. *J. Electrochem. Soc.* **2010**, *157*, A702.

(16) Perdew, J. P.; Wang, Y. Pair-Distribution Function and Its Coupling-Constant Average for the Spin-Polarized Electron Gas. *Phys. Rev. B* **1992**, *45*, 13244.

(17) Perdew, J. P.; Chevary, J. A.; Vosko, S. H.; Jackson, K. A.; Pederson, M. R.; Singh, D. J.; Fiolhais, C. Atoms, Molecules, Solids, and Surfaces: Applications of the Generalized Gradient Approximation for Exchange and Correlation. *Phys. Rev. B* **1992**, *46*, 6671.

(18) Venkatraman, S.; Manthiram, A. Investigation of the Possible Incorporation of Protons into Oxide Cathodes during Chemical Delithiation. *J. Solid State Chem.* **2004**, *177*, 4244.

(19) Benedek, R.; Thackeray, M. M.; Van De Walle, A. Pourbaix-like Phase Diagram for Lithium Manganese Spinels in Acid. *J. Mater. Chem.* **2009**, *20*, 369.

(20) Fang, C. M.; de Wijs, G. A. Local Structure and Chemical Bonding of Protonated $Li_xMn_2O_4$Spinels from First Principles. *Chem. Mater.* **2006**, *18*, 1169.

(21) Straatsma, T. P.; Berendsen, H. J. C. Free Energy of Ionic Hydration: Analysis of a Thermodynamic Integration Technique to Evaluate Free Energy Differences by Molecular Dynamics Simulations. *J. Chem. Phys.* **1988**, *89*, 5876.

(22) Hummer, G.; Pratt, L. R.; García, A. E. Free Energy of Ionic Hydration. *J. Phys. Chem.* **1996**, *100*, 1206.

(23) Tissandier, M. D.; Cowen, K. A.; Feng, W. Y.; Gundlach, E.; Cohen, M. H.; Earhart, A. D.; Coe, J. V.; Tuttle, T. R. The Proton's Absolute Aqueous Enthalpy and Gibbs Free Energy of Solvation from Cluster-Ion Solvation Data. *J. Phys. Chem. A* **1998**, *102*, 7787.

(24) Wang, Y. G.; Lou, J. Y.; Wu, W.; Wang, C. X.; Xia, Y. Y. Hybrid Aqueous Energy Storage Cells Using Activated Carbon and Lithium-Ion Intercalated Compounds. III. Capacity Fading Mechanism of $LiCo_{1/3}Ni_{1/3}Mn_{1/3}O_2$ at Different pH Electrolyte Solutions. *J. Electrochem. Soc.* **2007**, *154*, A228.

(25) Rao, M. M.; Jayalakshmi, M.; Schaf, O.; Wulff, H.; Guth, U.; Scholz, F. High-Temperature Combustion Synthesis and Electrochemical Characterization of $LiNiO_2$, $LiCoO_2$ and $LiMn_2O_4$ for Lithium-Ion Secondary Batteries. *J. Solid State Electrochem.* **2001**, *5*, 50.

(26) Benedek, R.; Thackeray, M. M.; Van De Walle, A. Free Energy for Protonation Reaction in Lithium-Ion Battery Cathode Materials. *Chem. Mater.* **2008**, *20*, 5485.